



UNITED NATIONS
UNIVERSITY

UNU-GTP

Geothermal Training Programme

Orkustofnun, Grensasvegur 9,
IS-108 Reykjavik, Iceland

Reports 2017
Number 11

GEOHERMAL EXPLORATION IN GRAENDALUR VALLEY, HVERAGERDI, S-ICELAND

Andualem Eshetu Gemechu

Geological Survey of Ethiopia

P.O. Box 2302

Addis Ababa

ETHIOPIA

andugech@gmail.com

ABSTRACT

Geothermal mapping was conducted in Graendalur valley, which is located north of Hveragerdi town, South Iceland. The area is at the eastern margin of the Western Volcanic Zone (WVZ) and the South Iceland Seismic Zone (SISZ). The geothermal activities are related to the SISZ and the older part of Hengill central volcano (Hveragerdi volcanic system). The scope of this study was to map all surface geothermal manifestations, alterations, soil temperatures, and the emission of CO₂ from the ground in order to examine the relationship between geothermal manifestations and structures. Then the results were compared with previous works in 1995 and 2009 to know whether changes occurred after the earthquakes in 2008. During the survey more than 217 geothermal manifestations were documented and 81 CO₂ and soil measurements took place. The geothermal manifestations mapped are fumaroles/steam vents, mud pools, warm to hot springs, warm to steaming grounds and mineral precipitations. The results show the presence of thermal fluid circulation near the surface. Thermal fluid movement is governed by sub surface structures trending NE-SW, N-S and NW-SE. The earthquake in 2008 formed some new geothermal activity and increased the existing activities. In the Graendalur valley new activities are still occurring.

1. INTRODUCTION

1.1 Study area and background

Graendalur geothermal field, is located approximately 6 km north of Hveragerdi town, which is located about 45 km south east of Reykjavik, the capital city of Iceland. The area is situated within the western part of the South Iceland Seismic Zone (SISZ), where it connects with the western flank of the active plate boundary between the North American and Eurasian plates (Figure 1).

The geothermal activity of the Graendalur geothermal field is related to the extinct Hveragerdi central volcano, which is one part of the Hengill volcanic system. Due to the extension of the plate boundaries, the Hveragerdi volcanic system has drifted away from the main rift (Ingólfsson et al., 2008; Arnórsson, 1995a in Munasinghe, 2013).

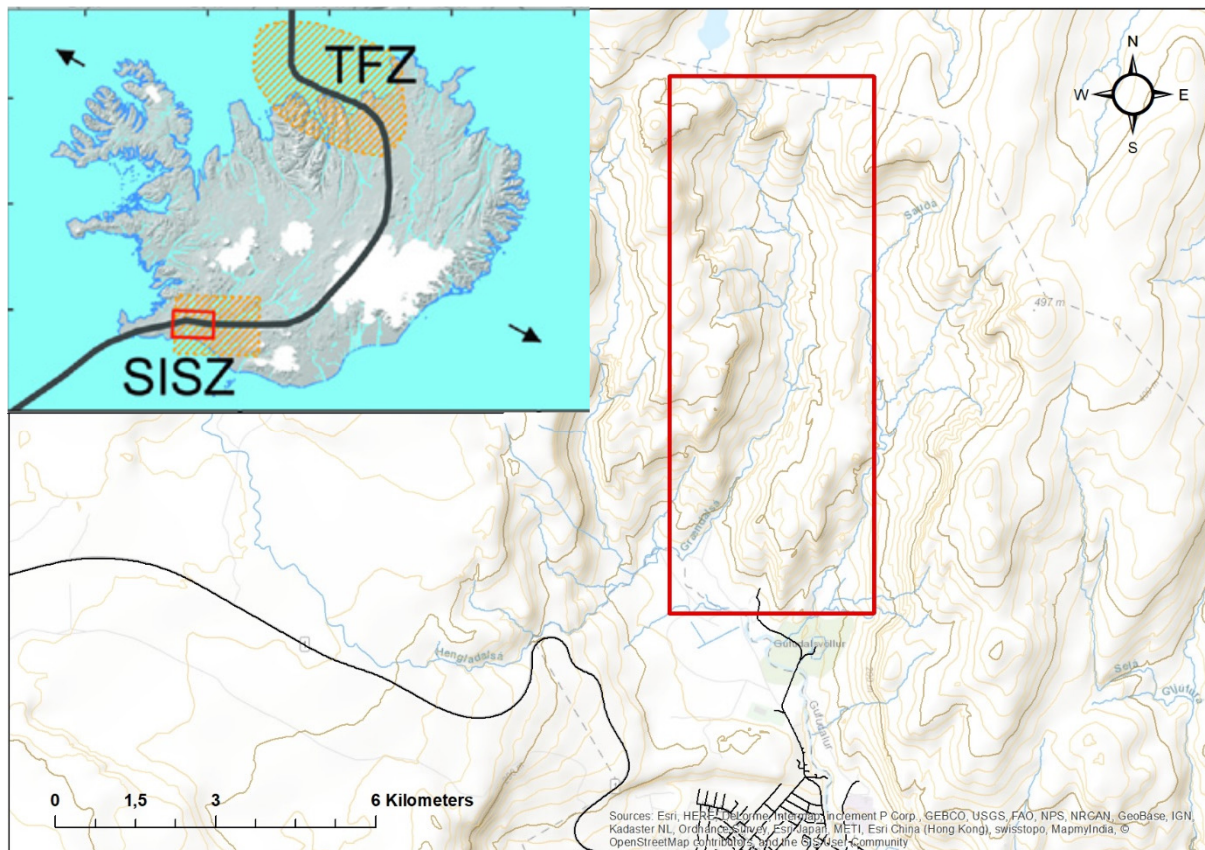


FIGURE 1: Location map of Graendalur geothermal field

Earthquakes with epicentres in the mapping area are quite common, due to its location within the SISZ. Lower intensity earthquakes (less than a magnitude of 4 on Richter scale) are common and larger earthquakes (magnitude up to 6 and above) occur regularly. The most recent large earthquake occurred on May 29th 2008 with a magnitude of 6.3, with the shocks causing major changes in the surface geothermal activity (Halldórsson and Sigbjörnsson, 2009).

The scope of this study was to map all surface geothermal manifestations, alterations, soil temperatures, and the emission of CO₂ from the ground in order to correlate the manifestations with geological structures. Then finally, the results were compared with previous works (Saemundsson, 1995a and b) and (Thorbjörnsson et al. 2009) to evaluate changes caused by the earthquakes in 2008.

1.2 Tectonic setting of Iceland

Iceland is located on constructive plate margin, between the Eurasian and North American plates (Saemundsson, 1979). Tectonic activity in the country is controlled by the interaction between the Icelandic mantle plume and the Mid-Atlantic Ridge with a spreading rate of 1.9 cm/y. In the northern and southern part of the country, the spreading is discontinuous as a result of the effect of an underlying hot spot located beneath the spreading ridge. The rift axis trends NE-SW across the country (Pedersen et al., 2003). As a result, the tectonic activity is exposed as a complex series of segments with active volcanic centres and fissure zones. The axial rift zone is categorized by several volcanic centres. The volcanic rift zones are connected to the Mid-Atlantic ridge across transform faults both in the north and south of Iceland known as Tjörnes fracture zone and SISZ respectively, and these zones are seismically very active. In the south of Iceland, the Reykjanes segment of the Mid Atlantic Ridge comes on shore at the Reykjanes peninsula forming an oblique rift zone, which merges with the Western Volcanic Zone (WVZ) (Saemundsson, 1979; Einarsson, 1991; Einarsson, 2008; Ziegler et al., 2016) (Figure 2).

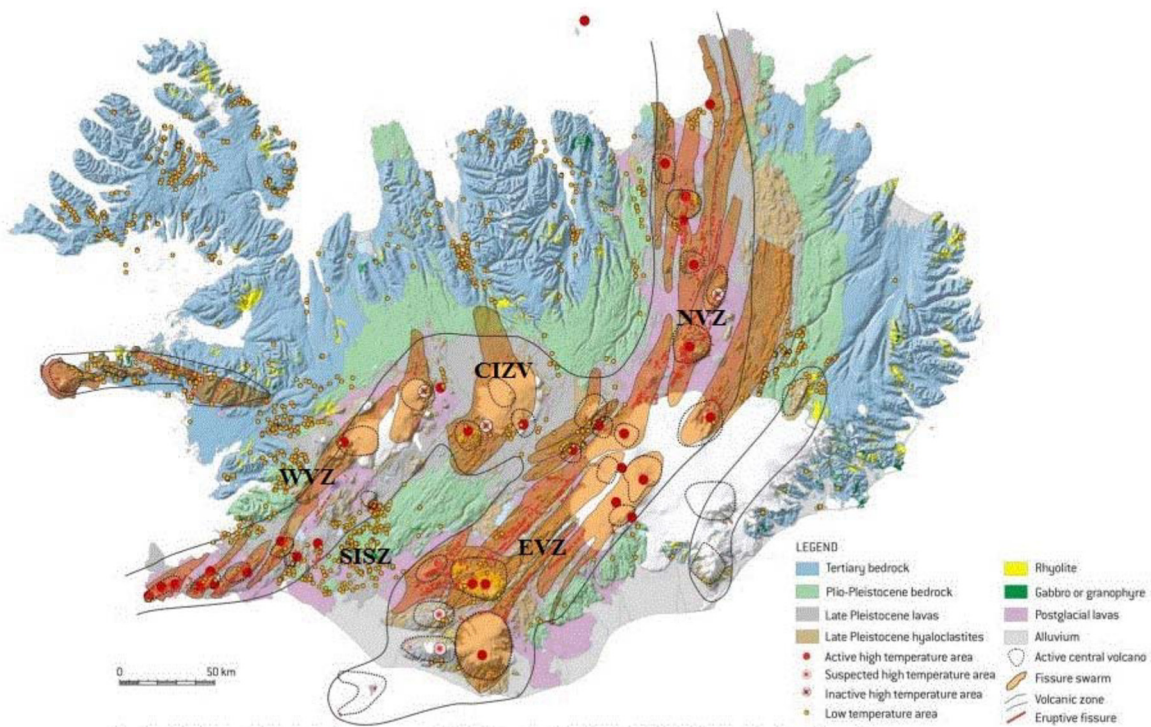


FIGURE 2: Geological and structural map of Iceland (Jóhannesson and Saemundsson, 1999)

1.3 Geothermal activity of Iceland

Based on the temperature and geological setting, the geothermal systems in Iceland are classified into two categories, low-temperature fields (with temperatures below 150°C at 1 km depth) and high-temperature fields (with temperatures above 200°C within 1 km depth). The high-temperature fields are related to central volcanos but low-temperature systems are located outside the rift zone in the Quaternary and Tertiary formations (Arnórrsson, 1995). In Iceland, both types of geothermal systems are utilized, the high-temperature fields are mainly used for electric power production but also for district heating, while low-temperature geothermal energy is used for space heating, fish farming, greenhouses, dairy products and spas.

1.4 South Iceland Seismic Zone (SISZ)

The South Iceland Seismic Zone is a transform fault zone and is a part of the Mid-Atlantic Ridge, which defines the boundaries between the North-American and Eurasian plates. The main faults are NNE-SSW right lateral faults and ENE-WSW left lateral faults. In addition to this, NE-SW, NW-SE and WNW-ESE trends are also observed in aerial photographs and in the field (Bergerat et al., 1998) (Figure 3). Historical records indicate that more than 30 periods of destructive earthquakes have been recorded in the SISZ since AD 1164, both through single and sequential events. Large earthquakes with a magnitude of 6 to 7 on a Richter scale have occurred every 45 to 112 years. Major destructive earthquakes have taken place in the SISZ, most of them of magnitude 6 and above. In 1896, five events were recorded in a period of two weeks with an estimated magnitude of 6-6.9. In 1912, a large earthquake occurred at the eastern border of the SISZ with a magnitude of 7 (Pedersen et al., 2003). In 2000, two large earthquakes were recorded in the SISZ. On June 17th an earthquake with a magnitude of 6.5 occurred and four days later, on June 21st, another 6.5 earthquake occurred. These events did increase the activity of geothermal manifestations (Pedersen et al., 2003).

The most recent large earthquake event in the SISZ happened on the 29th of May 2008 (Figure 3). The first earthquake had a magnitude of 6.3. The epicentre was east of farm Akurgerdi, between the towns of Selfoss and Hveragerdi, and the fault was N-S trending. Subsequently, another earthquake occurred, about 4 km west of the first earthquake. The epicentre of the second earthquake was on a N-S trending fault about 8 km west-northwest of Selfoss town, and about 2 km east of the town of Hveragerdi (Halldórsson and Sigbjörnsson, 2009).

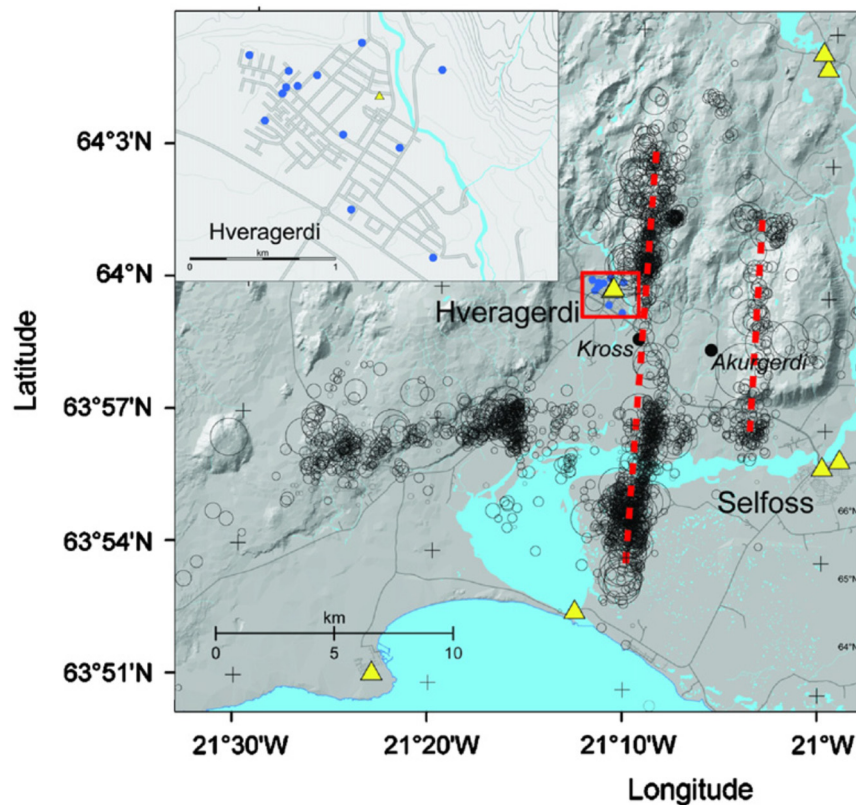


FIGURE 3: N-S trending alignment of the seismicity distribution for the period of 29 May to 29 June, 2008 in the South Iceland Seismic Zone. The circles indicate earthquakes (Halldórsson and Sigbjörnsson, 2009)

1.5 Hengill central volcano

Hengill central volcano is located about 30 km southeast of Reykjavik. The volcanic centre is located where the Reykjanes Peninsula, the South Iceland Seismic Zone and the Western Volcanic Zone form a triple junction. The Hengill volcanic area is generally classified into three systems, the oldest part is the Hveragerdi system, then the Hrómundartindur system and the youngest one being the Hengill system. (Ingólfsson et al., 2008, in Jousset et al., 2011; Saemundsson, 1967).

1.6 General geology of the Graendalur area

In Graendalur area, in relation with local tectonic activity, faulting and fractures are fairly common, trending predominantly NE-SW. Most of the fractures seen on surface are oriented NE-SW, NW-SE and N-S.; they have a displacement from the order of mm to cm, and, additionally, veins are filled by secondary minerals in areas of strong alteration. The tilting of the layers is common, anywhere between 2° to 8°, with the tilting increasing towards northwest. It is caused by progressively increased burial by the younger volcanism in the rift zone. The rocks in the study area are mainly composed of various lithofacies of subglacially formed hyaloclastites, interglacial lava flows and surface deposits. Most of the rocks are of basaltic composition, ranging from picrite, through olivine tholeiite to tholeiites, while basaltic andesites also occur. Petrographically the rocks range from glassy tuffs, through hyalocrystalline tuffs to porphyritic tuffs and also from aphyric fine- or coarse-grained rocks to various porphyritic rocks. Rock formations in the study area are listed in a downward chronological order as follows; Varmár formation, tholeiitic lavas, Kvíar basalt group (lavas foresets), stream deposits and rock slides, as shown in Figure 4 (Saemundsson and Fridleifsson, 1992).

Lithological units

Varmár formation (vm on map): It is a subglacial hyaloclastite formation; three rock units are well-known:

- Hyaloclastite breccia with lava pods forms the core of the formation, characterised by basalt pods and jointed basalt blocks with tuffaceous matrix. The lava pods are elongated N-S, the columnar jointing is irregular and compositionally they are a very fine-grained, dense, olivine free basalt, and they have tholeiitic composition.
- Hyaloclastite tuffs, composed of tuff or tuff-rich breccia, they are vesicular and relatively coarse in texture without being brecciated, showing a fairly typical expanded tholeiitic hyaloclastite-tuff. The glass is quite altered.
- Lava flows.

Tholeiitic lavas: This is an interglacial lava formation, exposed in the southwest part of the study area, composed of fine-grained aphyric tholeiitic texture exposed as irregularly columnar jointed basalts, which are dipping 2-3° to the south.

Kvíar basalt group: This is an interglacial lava formation, composed of lava units and breccia with a feldsparphyric texture and often exceptionally large feldspar phenocrysts are found.

Stream deposits: These are found above some of the largest rock slides, but the largest one is on the lowland in front of the valleys, where it partly covers the Holocene lava flows.

Rock slides: These are prominent surface features and cover a large part of the study area. All are from Holocene while their exact age is uncertain, but they are definitely slides due to the large earthquakes related to the SISZ.

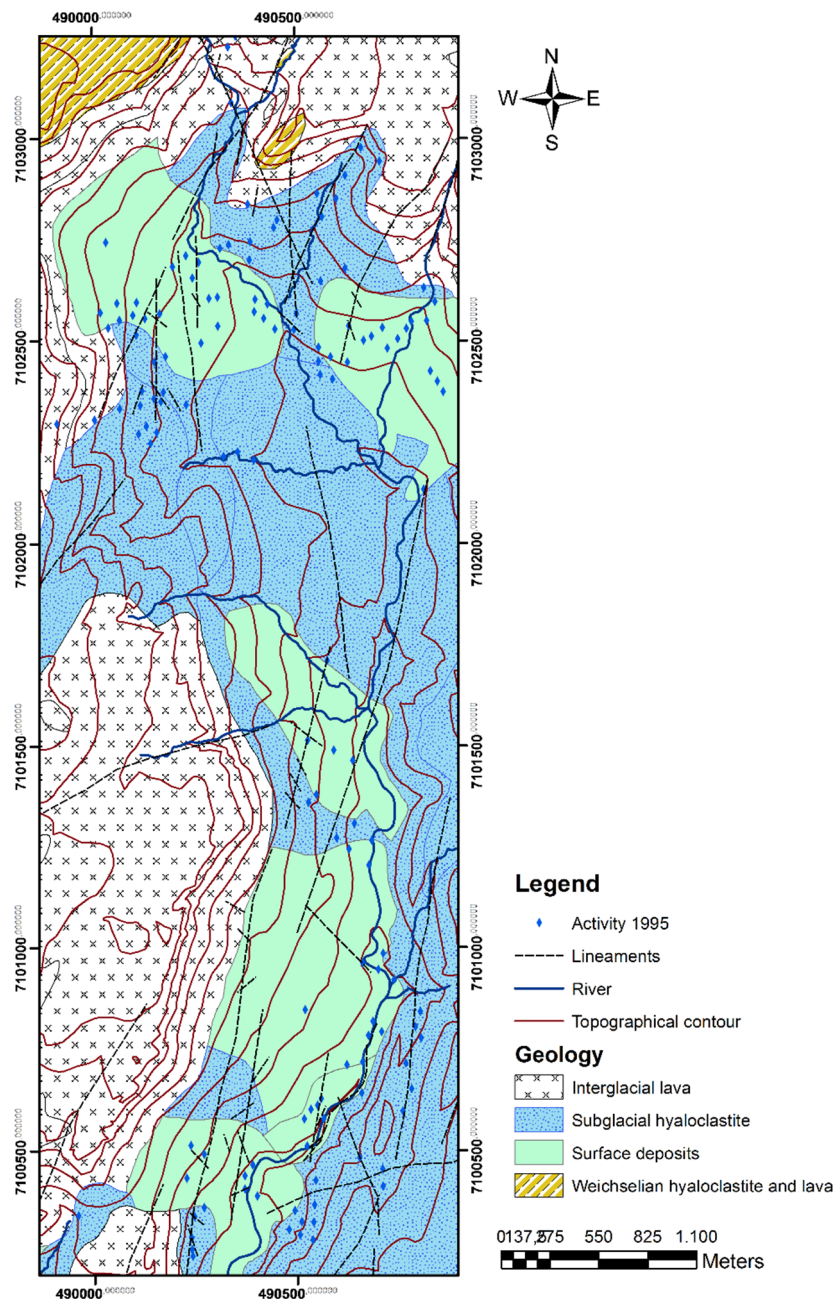


FIGURE 4: Lithological map of Graendalur valley

In the study area, hydrothermal clay-mineral zones are identified for rock alteration seen in the valley, characterized by greenish colours. This is due to mixed layer clays of smectite-chlorite (formed at temperatures $> 200^{\circ}\text{C}$), or chlorite (formed at temperature $>240^{\circ}\text{C}$). In the western side of the valley, rock alteration is characterized by black or dark brown colours due to smectite clay alterations (Saemundsson and Fridleifsson, 1992).

1.7 Previous work

Organised mapping of the Hengill and Hveragerdi area was first carried out in 1967 (Saemundsson, 1967). Subsequently in the area, geological and geothermal mapping was carried out in relation to drilling activities in Hveragerdi (Saemundsson and Arnórsson, 1971). Based on these two surveys, the Hveragerdi central volcano was outlined and many of the formations from which it is composed were mapped. In 1987, the Graendalur-Reykjadalur area was mapped by a UNU fellow (Wangombe, 1987). Jónsson (1989) undertook some research in the area, mostly on Upper Pleistocene and Holocene lavas. During 1989 and 1990, the geological mapping of this area was completed, the emphasis being on the lithostratigraphy, tectonics, the geothermal activity and alteration of the area (Saemundsson and Fridleifsson, 1992 and 1996). The maps were later combined with maps of the Hengill central volcano and published (Saemundsson, 1995a and b). Walker (1992) mapped the Hveragerdi volcano with respect to its eruptive units and their petrology. Geirsson and Arnórsson (1995) did a conceptual model of the Hveragerdi geothermal reservoir, based on chemical data from the surface. All this work was combined in a map of the Hengill central volcano at a scale of 1:50,000 (Saemundsson, 1995a). Geothermal exploration of the Hveragerdi-Graendalur area was also done by a UNU fellow (Kyagulanyi, 1996) and in the same year, geothermal exploration of the Saudá valley north of Hveragerdi was done by another UNU fellow (Malik, 1996). Kristjánsson and Fridriksson (2003) published a geothermal map of the Ölfus area, partly based on research done by Saemundsson, 1993a and b. Heat measurements in the soil and fractures in Hveragerdi were completed by Saemundsson and Kristinsson (2005). Thorbjörnsson et al. (2009) investigated the effects of the earthquakes of 29th May 2008 on the groundwater level, geothermal activity, fractures and pressure in boreholes in the Hveragerdi area. Finally, a UNU fellow (Munasinghe, 2013) did additional geothermal exploration of the Hveragerdi-Gufudalur area.

2. MAPPING OF GEOTHERMAL MANIFESTATIONS AND SOIL GAS MEASUREMENTS

2.1 Methodology

In the Graendalur - Hveragerdi valley, geothermal manifestations are in the form of warm to boiling springs, fumaroles/steam vents, warm to hot ground, mud pools and hydrothermal mineral precipitation. Soil temperature and soil gas (CO_2) measurements were carried out in a measurement grid to obtain information to determine the temperature distribution and CO_2 emissions from the ground. Subsequently, the result was to be correlated with research results obtained before and after the 2008 earthquake.

Methods and equipment used to measure the geothermal activity were: a GPS instrument, thermometer, CO_2 flux meter, compass, hand lens, hammer, digital camera and other writing tools. The thermometer was used to measure temperature in and at the manifestations and also ground temperature. The thermometer's probe was inserted into the ground and kept there for few minutes or until the measuring unit was acceptable to acquire the maximum temperature value. The location of each data point was recorded by the GPS instrument, and additionally, temperature values over 15°C were tracked and the location recorded. Subsequently the data obtained was downloaded into a computer after field work and plotted using *ArcGIS* software. Altered grounds were identified and mapped, including mineral precipitates from the altered grounds and hot springs, and samples were collected and analysed using XRD.

2.2 Characteristics of geothermal manifestations

2.2.1 Springs

Geothermal manifestations are an indicator of a structural discontinuity and hydrothermal systems at depth. In the study area, 86 springs were identified. The springs have a wide range of temperature and according to their temperature they are classified into three groups.

Cold springs (a): springs with temperatures below 15°C. They are a good indication for the structural mapping. Four cold springs were identified, all of them are located on the western side of the study area, where the groundwater can flow towards the surface through the fractures and faults.



FIGURE 5: Warm spring in Graendalur valley and mineral precipitation

Warm springs (b): springs with temperatures between 15 and 50°C. In some of the warm springs white minerals have deposited around them. There, samples were selected for XRD analysis and the result indicates the presence of aragonite and calcite associated with magnesia (Figure 5 and Appendix I).

Hot springs (c): springs with temperature above 50°C. They are an indicator of greater geothermal activity, they have different colours that depend on the dissolved materials, for instance blue and sometimes grey to brownish muddy. Some of the springs show eruptive behaviour and produce steam with H₂S smell and almost all of the warm and hot springs flow to the Varmá River (Figure 6).



FIGURE 6: Hot spring in Graendalur valley

2.2.2 Fumaroles/steam vents and mud pools

Fumaroles and steam vents are driven by steam discharge from a hydrothermal system, they are well known, often with a hissing sound. They reach towards the surface through tiny cracks or long fissures, and are a good indicator for the presence of a structural discontinuity. Usually they discharge steam and gases with different compositions, the most common contents are water vapour, CO₂ and H₂S and other gases. Fumaroles that release H₂S gas and are surrounded by sulphide depositions are called solfataras. Mud pools are formed in high-temperature geothermal fields, they are predominantly related to extremely high alteration and often display a light to dark grey colour (Figure 7).

2.2.3 Hydrothermal alteration, minerals, salt precipitation and warm grounds



FIGURE 7: Fumarole and mud pool in Graendalur valley

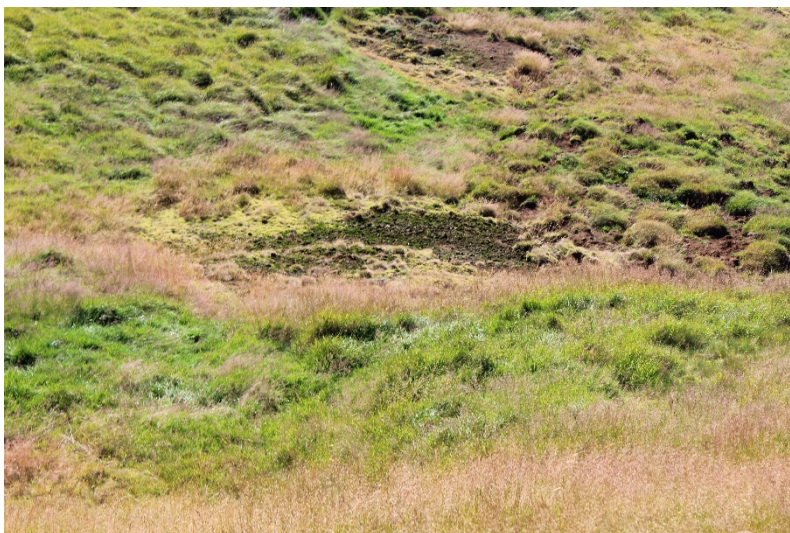


FIGURE 8: Yellowish green moss in warm ground in Graendalur valley

Due to the interaction of rock and hydrothermal fluid, the original rock changes its physical and chemical components by replacing primary minerals with secondary minerals. This process is called rock alteration. During the fieldwork, a number of temperature measurements were obtained in altered ground, they have a wide range of temperature difference, and based on the temperature measurement they are classified into two groups.

Warm ground where the temperatures are between 30 and 70°C. Warm grounds are often easily identified by bright yellowish or green moss vegetation cover, but if the temperature is below 30°C the ground is mostly covered by thick green grass (Figure 8).

Hot ground/steaming ground where the temperatures are above 70°C. This type of geothermal manifestations are recognized by wet, smooth, clay and mineral precipitation (Figure 9). They are shown as brownish-red, white or cream-white with scars of green-pale yellowish colour. Extinct or fossil alteration ground is identified, the original rock or soil changed to montmorillonite



FIGURE 9: Steaming ground in Graendalur valley

(smectite) clay minerals. For both warm and hot ground, mineral precipitations and hydrothermal mineral depositions, including clay samples from the extinct thermal alterations, four samples have been selected for XRD analysis and the result indicates the presence of gypsum, quartz and feldspar (Figure 9).

2.3 Soil gas measurements

CO₂ flux measurements were conducted in a grid of 800 m × 800 m, with 100 m between lines and measurements taken every 50 m on the line. A total of 81 data points were taken. CO₂-flux measurements were obtained by an automated CO₂-flux meter which uses the closed chamber method. The measuring unit contains a flux manager that records the CO₂ concentrations in ppm/s. It makes a slope and can be displayed on a smart phone. Shallow soil temperature measurements were taken in the same location as the CO₂ flux measurements. Both CO₂ and soil temperature data, including their coordinate location, were gridded using Golden Surfer software to produce a CO₂ and soil temperature contour map.

3. RESULTS

3.1 Relationship of the surface manifestations to the geologic structures

Geological structures like faults and fractures can be outlined by their lateral or vertical displacement and with their geomorphological appearance from field observations. Along the eastern and western side of the study area faults are exposed, with NE-SW, N-S and NW-SE directions, and show a 10-20 m displacement, but the remaining part of the area is covered by sediments and rock slide deposits. Thus, it was quite difficult to outline the structural discontinuities, but geothermal manifestations are exposed in this part of the area. The alignment of geothermal manifestations was therefore used as an indication for the presence of a structural discontinuity. While the prominent lineaments have directional trends of the manifestation, the lineaments may also indicate fracture zones or other geological conditions and lineaments are predominantly oriented similarly with faults in the western and eastern part of the study area.

3.2 Details of geothermal manifestations

During the field work, a number of temperature measurement were taken where the area contains a large number of manifestations and all the points were plotted on a map (Figure 10). They were divided into 10 localities which are described below. The map also contains previous geothermal exploration results, which were conducted in the area by Saemundsson (1995) and Thorbjörnsson et al. (2009) before and after the 2008 earthquake, respectively. As shown on the map in locality GR-07 and GR-10 there are new geothermal manifestations which were not identified in the 1995 and 2008 studies. And in localities GR-02, GR-05, GR-08 and GR-09 there are manifestations that occurred during the 2008 earthquake, but were not identified in the 1995 study.

In order to show the details of the geothermal manifestations on a map, classification is needed. Localities of the active areas are therefore grouped in three different maps.

3.2.1 Localities GR-01, GR-02, GR-03 and GR-04 (Figure 11)

Locality GR-01

This locality contains intense geothermal activities; the total area coverage is about 100 × 20 m² in size and extends along NNE-SSW. Exposed geothermal manifestations are hot and steaming ground, one boiling and three hot springs and two fumaroles with temperatures as high as 98°C. The steaming ground is surrounded by red-brownish, white and yellowish mineral precipitates (Figure 12).

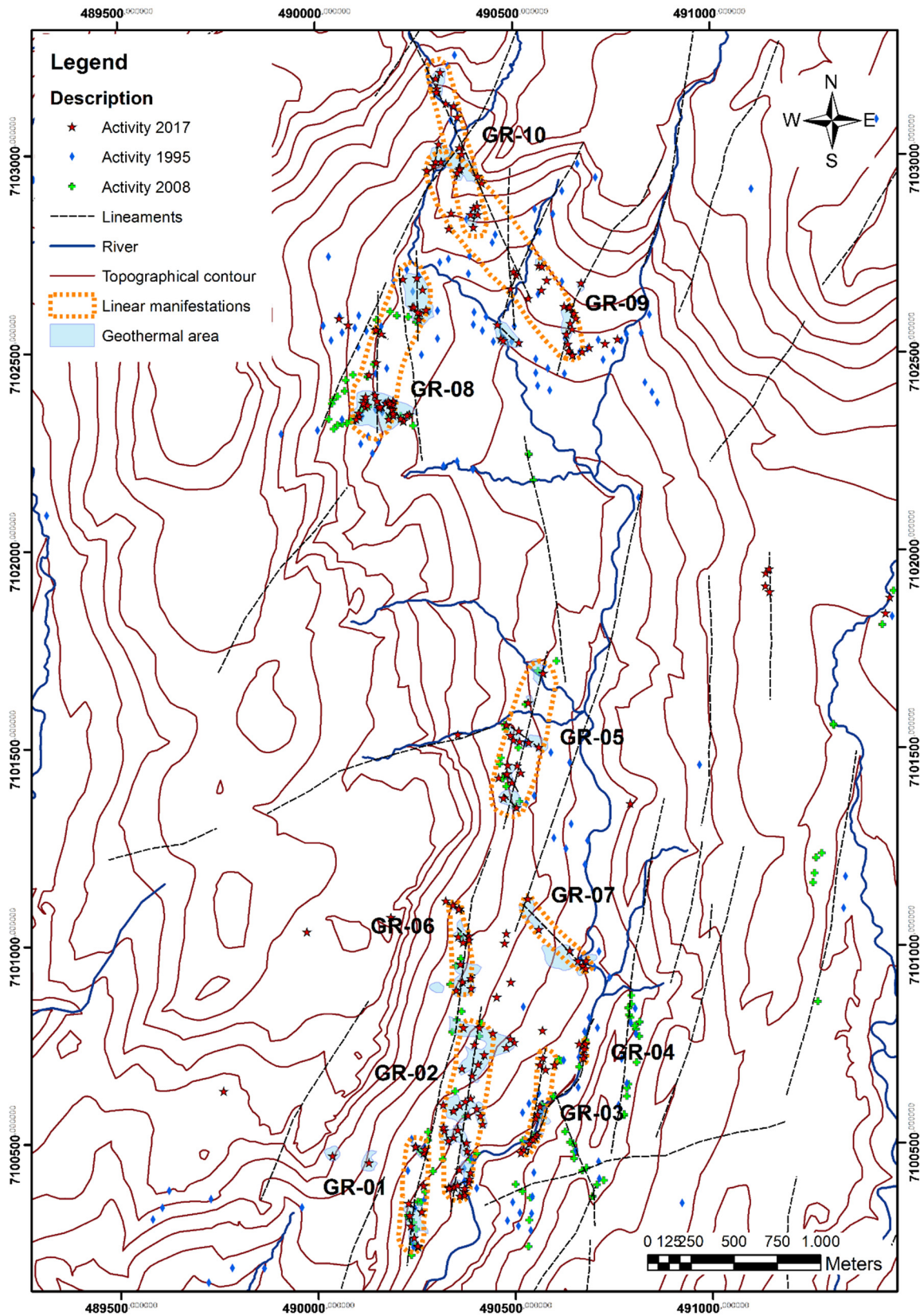


FIGURE 10: Map showing geothermal manifestations and structures; geothermal activities as mapped in 1995, 2008 and 2017 are shown in different colours; active geothermal areas are shown in 10 localities

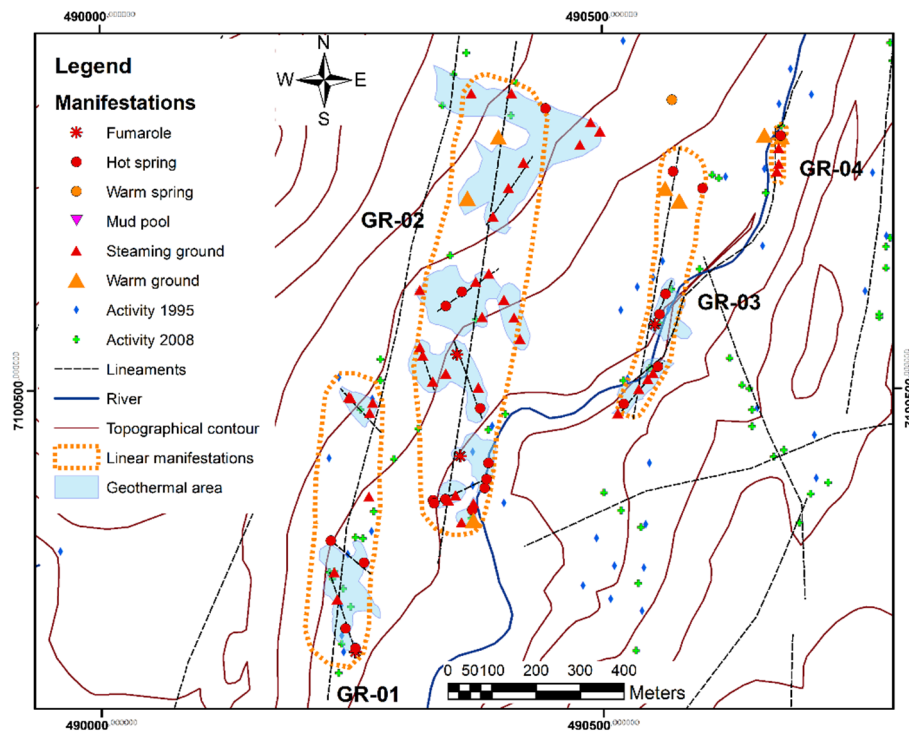


FIGURE 11: Map showing geothermal manifestations, structures and active geothermal areas in localities GR-01, GR-02, GR-03 and GR-04

Locality GR-02

In this locality a large number of geothermal manifestations are grouped. The total area coverage is approximately $210 \times 75 \text{ m}^2$ in size and includes a group of manifestations with a NE-SW trend. They are composed of steaming ground, surrounded by red-brownish, white and yellowish mineral precipitates. A sample selected from the steaming ground for XRD analysis indicates the presence of gypsum, quartz and feldspar minerals. Four fumaroles are found in this location, most of them within the steaming ground, ten hot springs and a circular mud pool with a diameter approximately 10 m, with low viscosity and light grey coloured. Around the northern part of locality GR-02 drying grass with yellowish green moss in the warm ground were identified, which is an indication of new geothermal activity. Based on the study from 1995, the geothermal activity has shifted eastwards, but comparisons with the 2008 study indicates that the geothermal activity has recently become wider.



FIGURE 12: Geothermal activity in locality GR-01

Locality GR-03

At this location the geothermal manifestations follow the direction of the Varmá River, and contained six major hot springs and two fumaroles. A sample selected for XRD analysis from around the fumarole



FIGURE 13: Geothermal activity in locality GR-03

indicates the presence of sulphur minerals. In the southern part of the locality, manifestations are exposed on a hill side (Figure 13). The steaming ground is surrounded by red-brownish, white and yellowish mineral precipitates with temperatures above 98°C and in the northern part of the locality wilted grass with yellowish green moss were identified, which is an indication of new geothermal activity.

FIGURE 13: Geothermal activity in locality GR-03
 geothermal manifestations follow a straight line with a NE-SW direction. At this locality, a comparison with the 1995 and 2008 records indicate that the areal extension of the geothermal activity has diminished.

Locality GR-04

In this locality there is strongly altered steaming ground covered with red to brownish, light greenish, white and yellow mineral precipitates, one hot spring and one warm spring. Sample selected for XRD analysis indicates the presence of aragonite and calcite associated with magnesium minerals.

3.2.2 Localities GR-05, GR-06 and GR-07 (Figure 14)

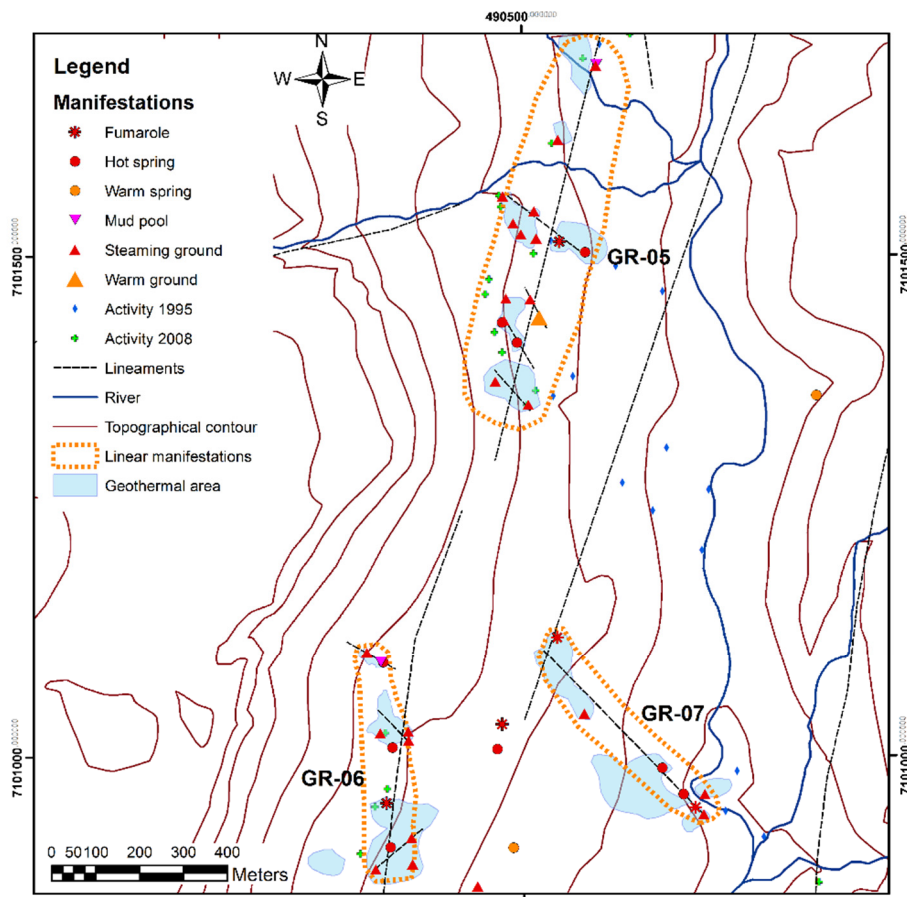


FIGURE 14: Map showing geothermal manifestations, structures and active geothermal areas in localities GR-05, GR-06 and GR-07

Locality GR-05

At this location a group of large boiling springs, boiling mud pools, and fumaroles were found, together with steaming ground and the area coverage is approximately $60 \times 10 \text{ m}^2$ with abundant mineral precipitations, hot and warm ground. A boiling spring with about a $2 \times 4 \text{ m}^2$ size pool was identified and the boiling spring was regularly raising the water level about 10-20 cm. Five boiling mud pools are distributed in this area surrounded by brownish and grey coloured clay. On the southern part of the locality is a hot spring with steaming ground surrounded by yellowish green moss vegetation (Figure 15).



FIGURE 15: Geothermal activity in locality GR-05

Locality GR-06

At this locality the manifestation is located on a steep slope with abundant boulder rock slides, and it contains six hot springs with temperatures around 98°C , two small mud pools and two fumaroles, and steaming ground with sulphur (H_2S) odour. The activity covers a circular area with a radius of 20 m, the vegetation is dying due to the hot and steaming ground. Yellowish green moss covers most of the warm ground (Figure 16).



FIGURE 16: Geothermal activity in locality GR-06

Locality GR-07

In this locality there are three centres of geothermal manifestation: They are placed along line with a NW-SE direction, and steaming ground is present with red to brownish colour and white mineral precipitation. The total area coverage is approximately $100 \times 20 \text{ m}^2$, two fumaroles, one strong sounding fumarole, a mud pool with circular diameter of approximately 1 m, three hot springs with a temperature above 96°C and one warm spring. Sample taken for XRD analysis indicates the presence of calcite minerals. Based on the previous work in 1995 and 2008, the geothermal activity here is new.

3.2.3 Localities GR-08, GR-09 and GR-10 (Figure 17)

Locality GR-08

At this locality, three major thermal manifestations are grouped together (Figure 18), with ten hot springs, five fumaroles, two mud pools and two warm springs recognised. The area contains a $6 \times 2 \text{ m}^2$ mud pool and red-brownish, white and yellowish mineral precipitates are abundant.

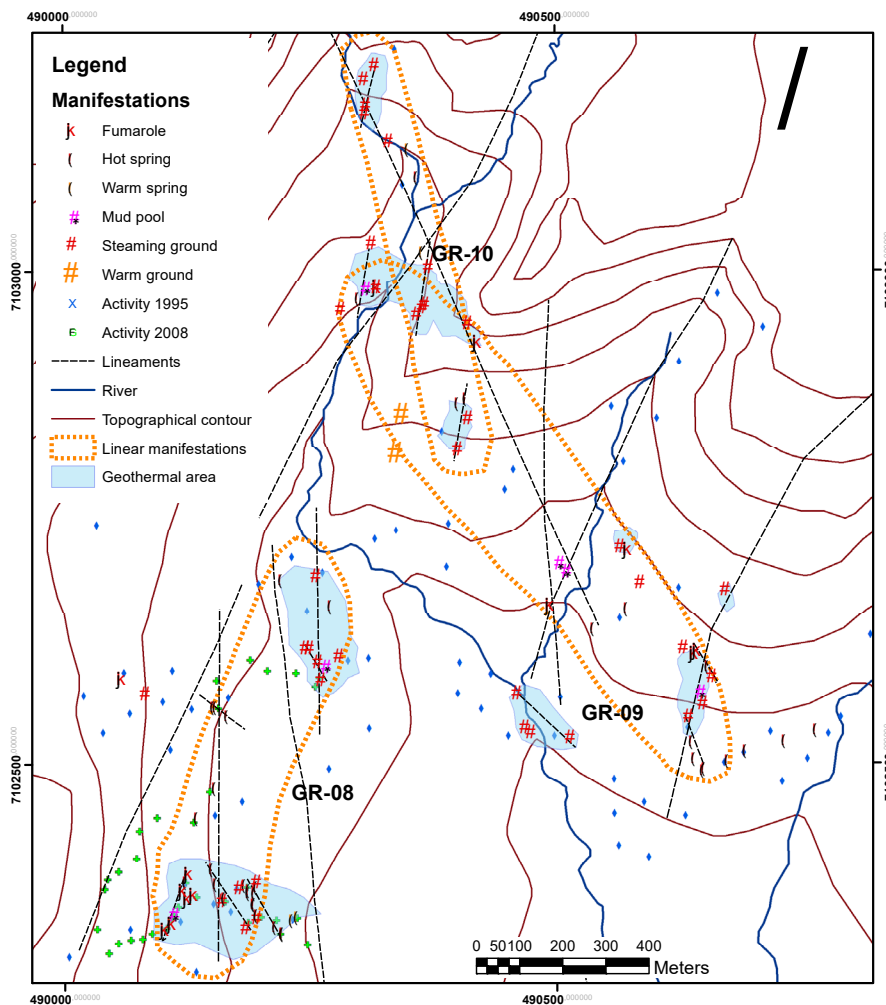


FIGURE 17: Map showing geothermal manifestations, structures and active geothermal areas in localities GR-08, GR-09 and GR-10



FIGURE 18: Locality GR-08

Locality GR-09

At this location, four boiling springs, and three mud pools were identified, but one of the big boiling mud pools had a strong discharging fumarole, around it. The rock or soil was changed to white yellowish and red clay material, and the mud was dark greyish. The boiling mud pool was circularly shaped and about 4 m in diameter with abundant mineral precipitations, as shown in Figure 7.

Locality GR-10

In this locality the geothermal activity is recent, based on previous work in 1995 and 2008. Large areas covered by hot and

steaming ground with temperatures greater than 95°C were concentrated around the river and also on top of the hill. Quite strong alteration was observed. Four hot springs and abundant warm springs are present. Most of them are intermixed with the river water. At the southern part of this locality, wilted grass or yellowish green moss vegetation were observed. In the northern part of the locality, an extinct alteration was observed and a sample selected for XRD analysis indicated the presence of smectite clay minerals (Figure 19).



FIGURE 19: Geothermal activity in locality GR-10

3.3 Soil gas measurements

The maximum value of CO₂ concentration recorded was 165.476 g/m²day, which was taken from a steaming ground, while the minimum value was 0.029 g/m²day. CO₂-flux measurements data with the coordinated locations were gridded using Golden Surfer software to produce a CO₂-flux contour map (Figure 20). Soil temperatures were processed in a similar way. The CO₂ emission and soil temperature measurement maps show CO₂ and soil temperature anomalies oriented along NE-SW, N-S and NW-SE directions (Figure 21).

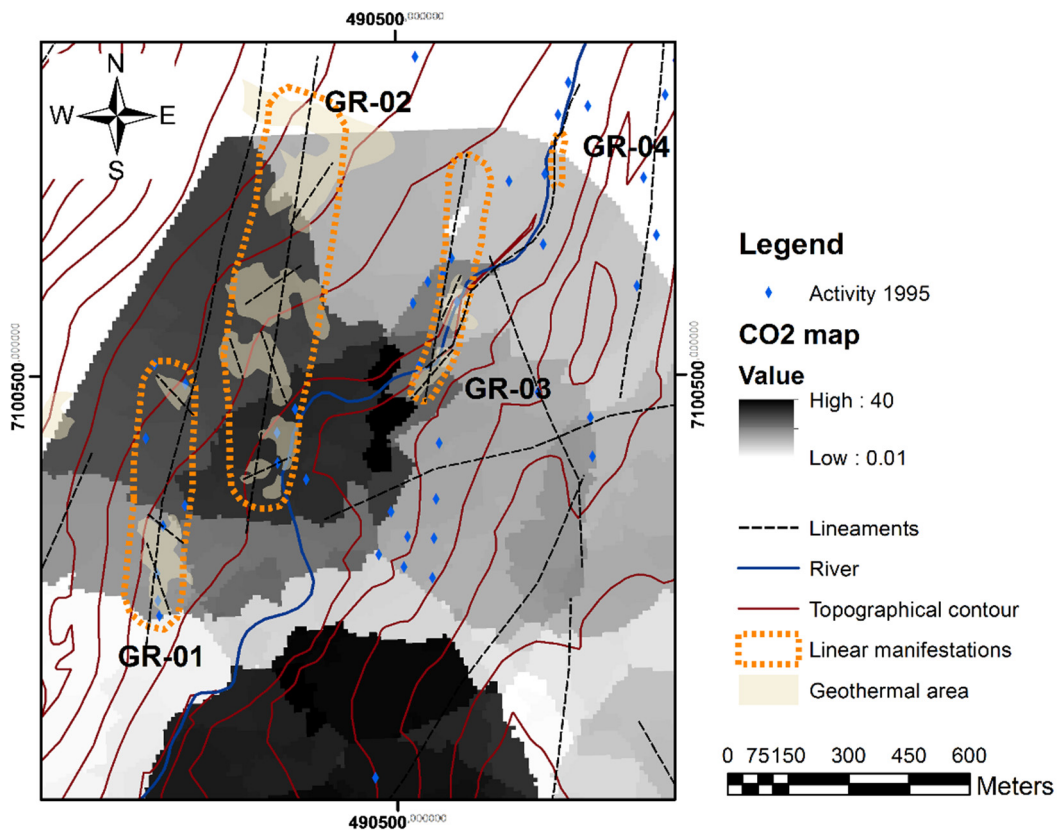


FIGURE 20: CO₂ emission map (g/m²day) of the measured area in Graendalur valley

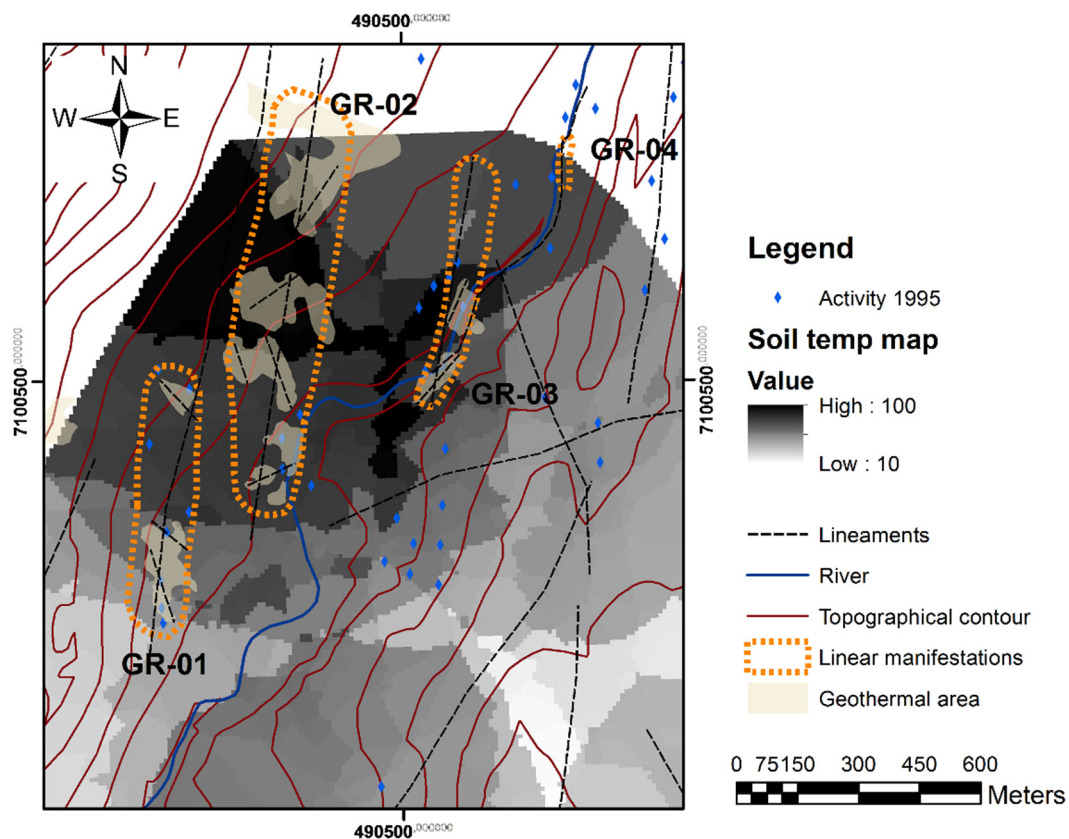


FIGURE 21: Soil temperature map (°C) of the measured area in Graendalur valley

4. CONCLUSIONS

- A linear alignment of geothermal manifestations is an indication of geological structures such as a fault or a fracture. This means that the geothermal manifestations are controlled by geological structures.
- Thermal fluid movement in the study area is governed by linear subsurface structures oriented along NE-SW, N-S and NW-SE directions.
- CO₂ emission and soil temperature measurement results confirm the structural patterns, which are outlined by the linear trend of manifestations to the NE-SW, N-S and NW-SE directions.
- XRD results indicate the presence of aragonite and calcite associated with magnesium minerals precipitations from springs, and gypsum, quartz, feldspar and sulphur mineral deposits for the steaming ground.
- The earthquakes in 2008 created new geothermal activity in the study area, with most of the existing geothermal activities also increasing. On the other hand, some other existing activities were subdued or became extinct after the earthquake. In the valley new activities are still occurring.

ACKNOWLEDGEMENTS

I would like to express my gratitude to the UNU-GTP and the Icelandic Government for funding my training; Mr Lúdvík S. Georgsson director of UNU-GTP, for giving me the opportunity to attend this training. I would also like to thank Mr. Ingimar G. Haraldsson, Ms. Málfríður Ómarsdóttir, Ms. Thórhildur Ísberg and Mr. Markús A.G. Wilde, for their kindness and efficient help throughout my stay in Iceland. My deepest thanks go to my supervisors, Sigurdur G. Kristinsson and Audur Agla Óladóttir and also to Anette K. Mortensen for their guidance and help both in the field and during the preparation of the report. I also want to thank the UNU-GTP Fellows of 2017 for our unforgettable relationship. Finally, I would like to thank my family and my friends for their support during these six months.

REFERENCES

- Arnórsson, S., 1995: Geothermal systems in Iceland: Structure and conceptual models II. Low-temperature areas. *Geothermics*, 24, 603-629.
- Bergerat, F., Gudmundsson, A., Angelier, J. and Rögnvaldsson, S.T., 1998: Seismotectonics of the central part of the South Iceland Seismic Zone. *Tectonophysics*, 298, 319-335.
- Einarsson, P., 1991: Earthquakes and present-day tectonism in Iceland. In: Björnsson, S., Gregersen, S., Husebye, E.S., Korhonen, H., and Lund, C.E. (editors), *Imaging and understanding the lithosphere of Scandinavia and Iceland*. *Tectonophysics*, 189, 261-279.
- Einarsson, P., 2008: Plate boundaries, rifts and transforms in Iceland. *Jökull*, 58, 35–58.
- Geirsson, K. and Arnórsson, S., 1995: Conceptual model of the Hveragerdi geothermal reservoir based on chemical data. *Proceedings of the World Geothermal Congress 1995, Florence, Italy*, 2, 1251-1256.
- Halldórsson, B., and Sigbjörnsson, R., 2009: The Mw6.3 Ölfus earthquake at 15:45 UTC on 29 May 2008 in South Iceland: ICEARRAY strong-motion recordings. *Soil Dynamics and Earthquake Engineering*, 29, 1073-1083.
- Ingólfsson, Ó., Sigmarsson, O., Sigmundsson, F., and Símonarson, L., 2008: The dynamic geology of Iceland. *Jökull*, 58, 1–2.
- Jóhannesson, H., and Saemundsson, K., 1999: *Geological map of Iceland 1:1.000.000. Náttúrufræðistofnun Íslands*.
- Jónsson, J., 1989: *Hveragerdi and surroundings, geological overview*. Rannsóknarstofnunin Nedri Ás, report 50 (in Icelandic), 56 pp and map.
- Jousset, P., Haberland, C., Bauer, K. and Árnason, K., 2011: Hengill geothermal volcanic complex (Iceland) characterized by integrated geophysical observations. *Geothermics*, 40, 1–24.
- Kristjánsson, B.R., and Fridriksson, Th., 2003: *State Horticultural School, Reykir in Ölfus. Geothermal map*. ISOR – Iceland GeoSurvey, report 2003-01(in Icelandic), 4 pp.
- Kyagulanyi, D., 1996: Geothermal exploration in the Hveragerdi Graendalur area, SW-Iceland. Report 8 in: *Geothermal training in Iceland 1996*. UNU-GTP, Iceland, 161-176.
- Malik, A.H., 1996: Geothermal exploration of Saudá valley north of Hveragerdi, SW-Iceland. Report 9 in: *Geothermal training in Iceland 1996*. UNU-GTP, Iceland, 177-195.

- Munasinghe, M.M.T.N.B., 2013: Geothermal exploration in Gufudalur, Hveragerdi, SW-Iceland. Report 21 in: *Geothermal training in Iceland 2013*. UNU-GTP, Iceland, 477-500.
- Pedersen, R., Jónsson, S., Árnadóttir, Th., Sigmundsson, F., and Feigl, K.L., 2003: Fault slip distribution of two June 2000 MW6.5 earthquakes in South Iceland estimated from joint inversion of InSAR and GPS measurements. *Earth and Planetary Science Letters*, 213, 487-502.
- Saemundsson, K., 1967: *Vulkanismus und Tektonik des Hengill-Gebietes in Sudwest-Island*. Acta Nat. Isl., II-7, PhD thesis (in German), 195 pp.
- Saemundsson, K., 1979: Outline of the geology of Iceland. *Jökull*, 29, 7-28.
- Saemundsson, K., 1993a: *Hveragerdi – geothermal activity*. Orkustofnun, Reykjavík, report KS-93/20, 33 pp.
- Saemundsson, K., 1993b: *Geothermal map of Hveragerdi and Reykir*. Orkustofnun, Reykjavík, report JHD-JFR8716, 54 pp.
- Saemundsson, K., 1995a: *Geological map of the Hengill area 1:50,000*. Orkustofnun, Reykjavík.
- Saemundsson, K., 1995b: *Geothermal and hydrothermal map of the Hengill area, 1:25,000*. Orkustofnun, Reykjavík.
- Saemundsson, K., and Arnórsson, S., 1971: *A report on well ASI-1 at Ölfusborgir in Ölfus*. Orkustofnun, Reykjavík, report (in Icelandic), 9 pp and figs.
- Saemundsson, K., and Fridleifsson, G.Ó., 1992: *The Hveragerdi central volcano, geological description*. Orkustofnun, Reykjavík, report OS-92063/JHD-35 B (in Icelandic), 25 pp.
- Saemundsson, K., and Fridleifsson, G.O., 1996: *The Hveragerdi central volcano. An extended English abstract from Saemundsson, K., and Fridleifsson, G.Ó., 1992: The Hveragerdi central volcano, geological description*. Orkustofnun, Reykjavík, report GOF-KS-96/03, 10 pp.
- Saemundsson, K., and Kristinsson, S.G., 2005: *Hveragerdi. Temperature measurements in earth and fractures*. ÍSOR – Iceland GeoSurvey, Reykjavík, report ISOR-2005/041 (in Icelandic), 16 pp + 2 maps.
- Thorbjörnsson, D., Saemundsson, K., Kristinsson, S.G., Kristjánsson, B.R, and Ágústsson, K., 2009: *Southern lowland earthquakes 29th May 2008. Effect on groundwater level, geothermal activity and fractures*. ÍSOR – Iceland GeoSurvey, Reykjavík, report 2009/028 (in Icelandic), 42 pp.
- Walker, C., 1992: *The volcanic history and geochemical evolution of the Hveragerdi region, SW Iceland*. University of Durham, Durham, PhD thesis, 356 pp.
- Wangombe, P.W., 1987: *Mapping at Graendalur - Reykjadalur area, Hveragerdi, SW Iceland*. UNU-GTP, Iceland, report 15, 26 pp.
- Ziegler, M., Rajabi, M., Heidbach, O., Hersir, G.P., Ágústsson, K., Árnadóttir, S. and Zang, A., 2016: The stress pattern of Iceland. *Tectonophysics* 674, 101-113

APPENDIX I: XRD measurements on samples from Graendalur valley

59693/UNU anduaalem #4

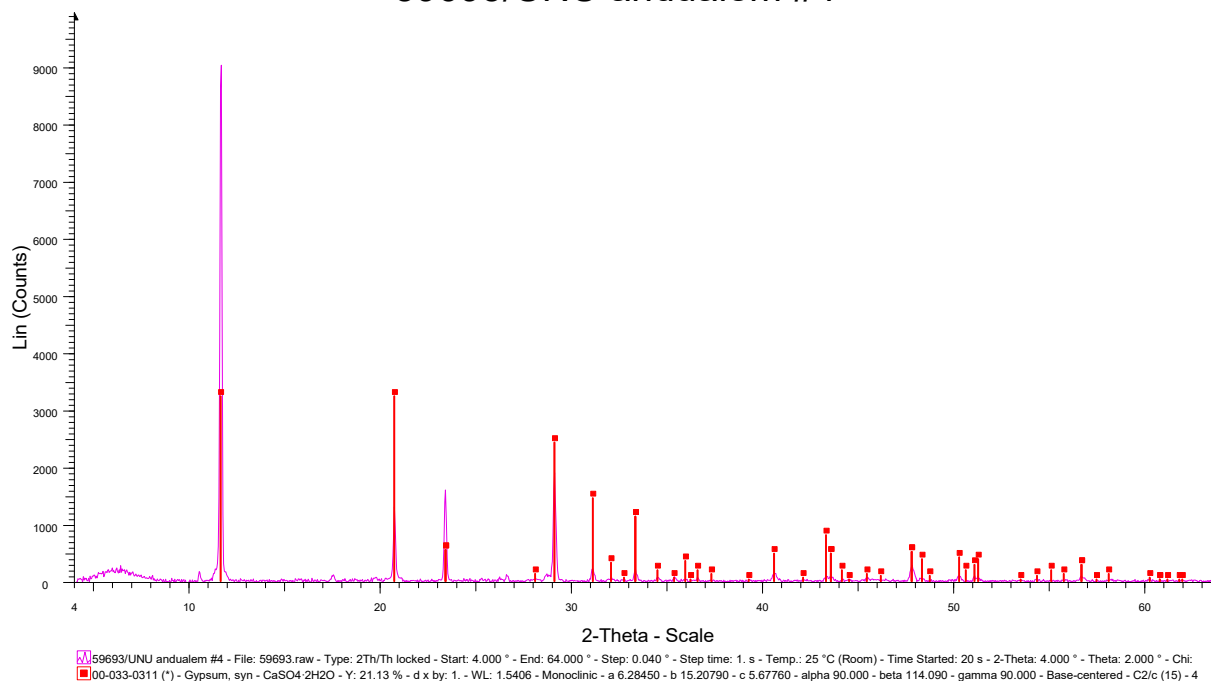


FIGURE 1: XRD graph indicating the presence of gypsum in sample 4 collected from steaming ground at locality GR-02

59694/UNU anduaalem #5

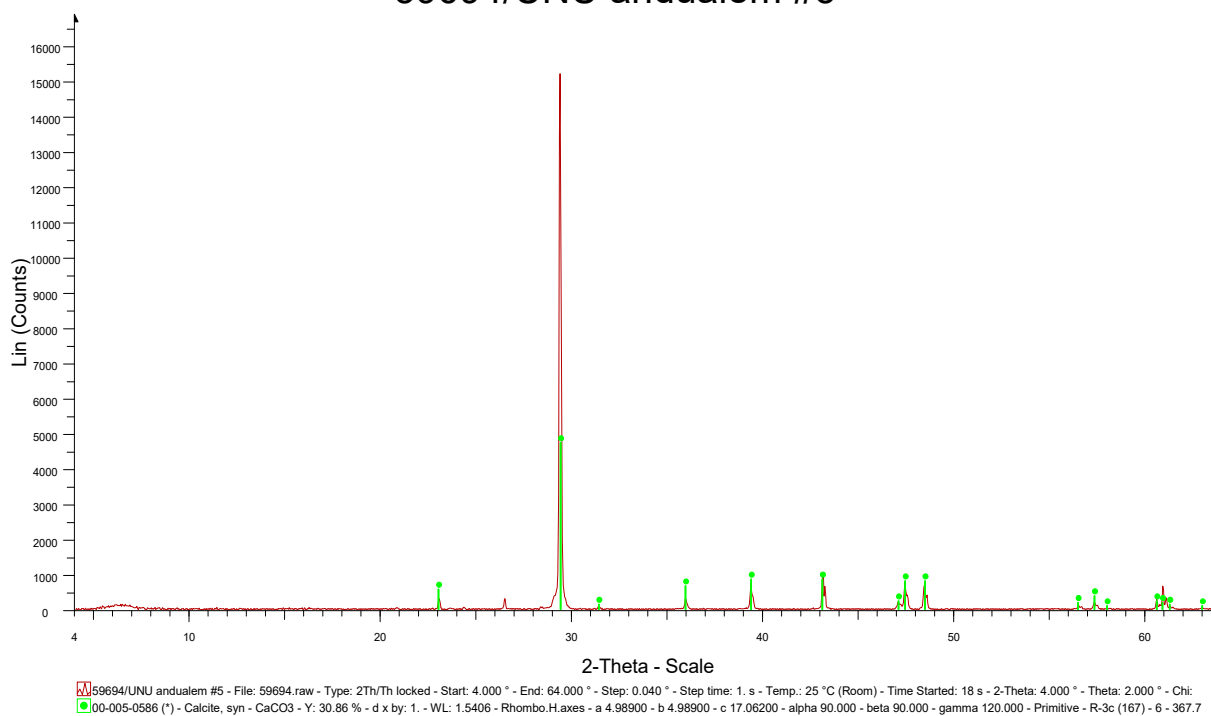


FIGURE 2: XRD graph indicating the presence of calcite in sample 5 collected from warm spring at locality GR-02

59695/UNU anduaalem #7

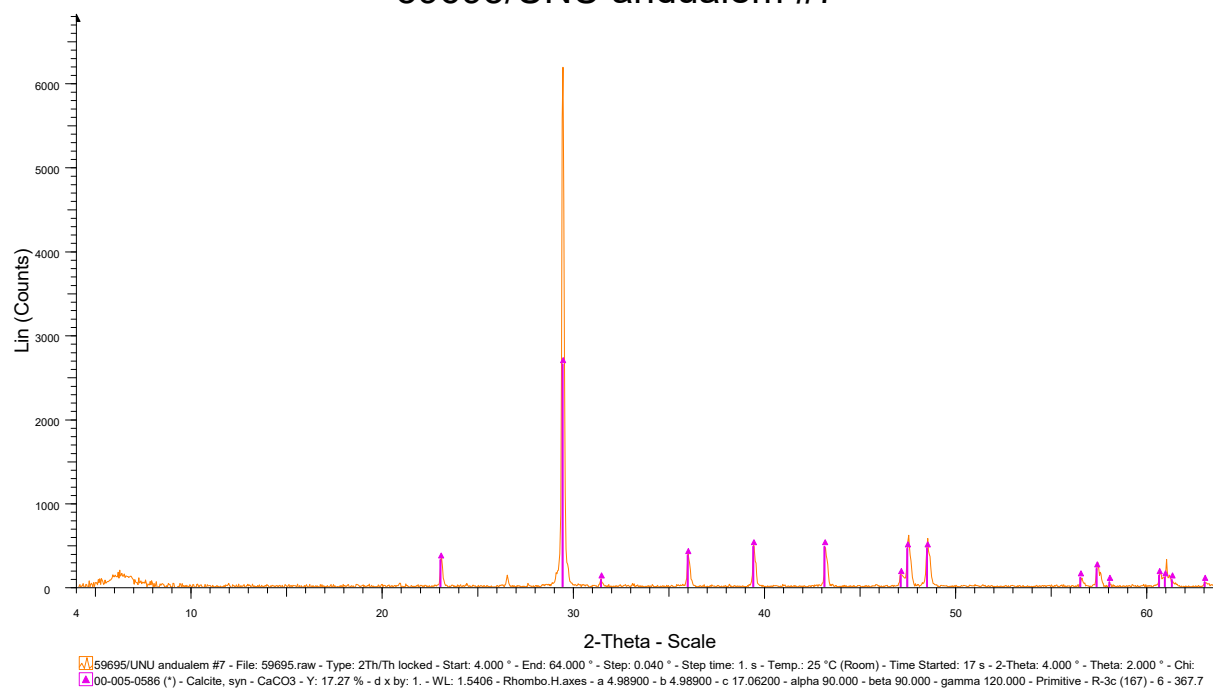


FIGURE 3: XRD graph indicating the presence of calcite in sample 7 collected from warm spring at locality GR-07

59696/UNU anduaalem #9

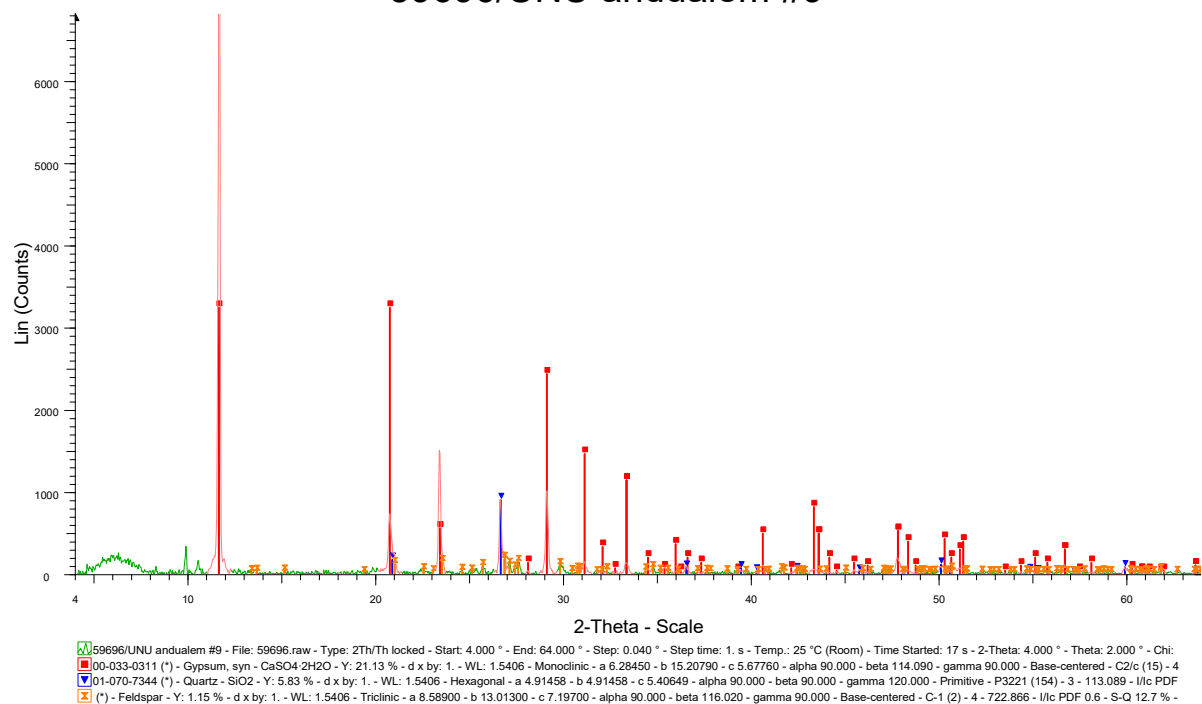


FIGURE 4: XRD graph indicating the presence of gypsum, quartz and feldspar in sample 9 collected from steaming ground at locality GR-04

59697/UNU anduaalem #10

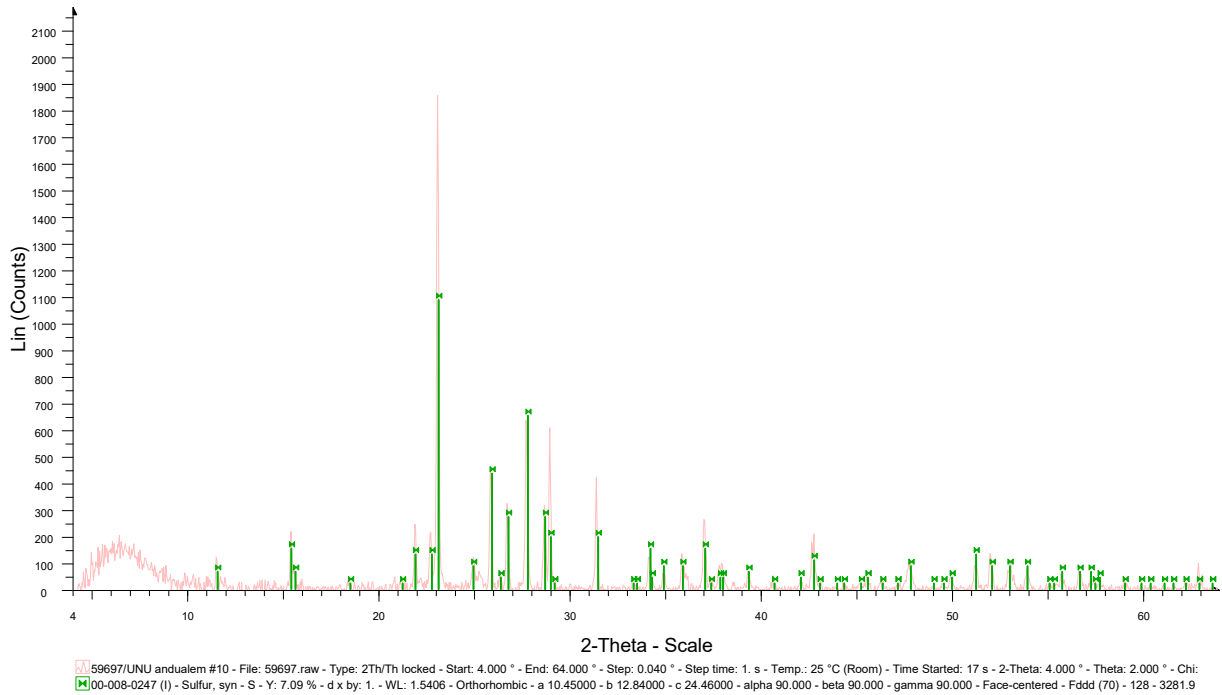


FIGURE 5: XRD graph indicating the presence of sulphur in sample 10 collected from around the fumarole at locality GR-03

59698/UNU anduaalem #11

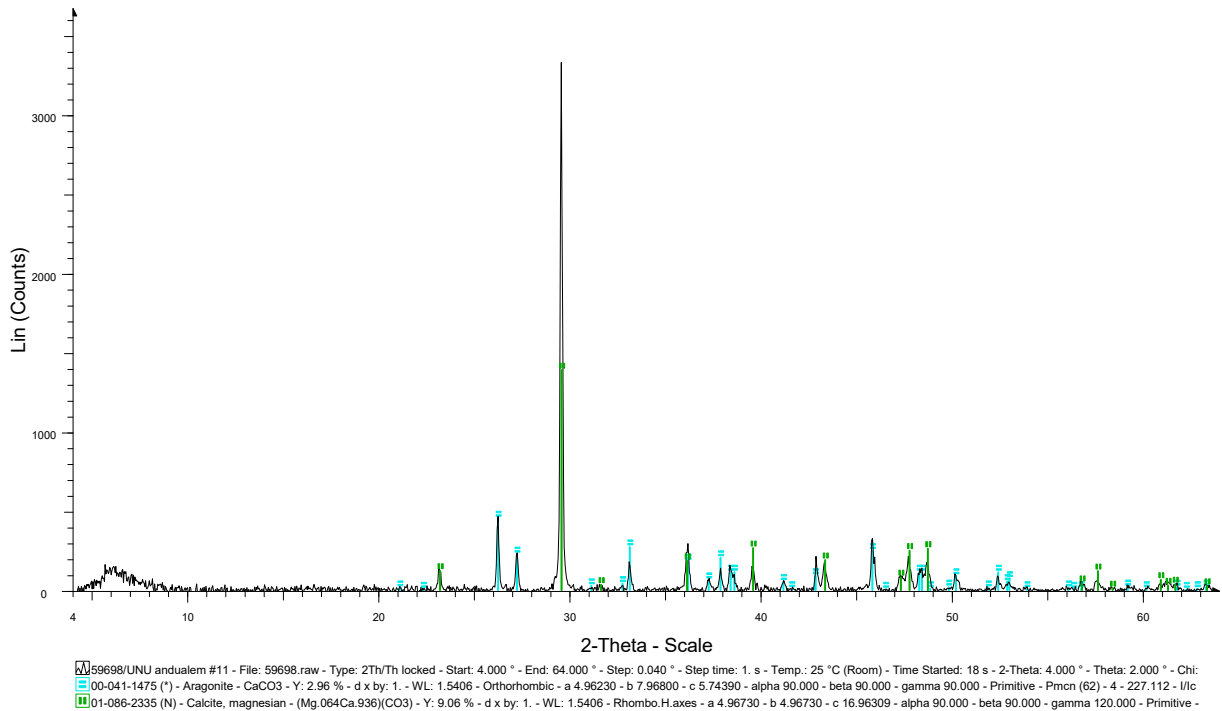


FIGURE 6: XRD graph indicating the presence of aragonite, calcite and magnesium in sample 11 collected from warm spring at locality GR-04

59699/UNU anduaem #12

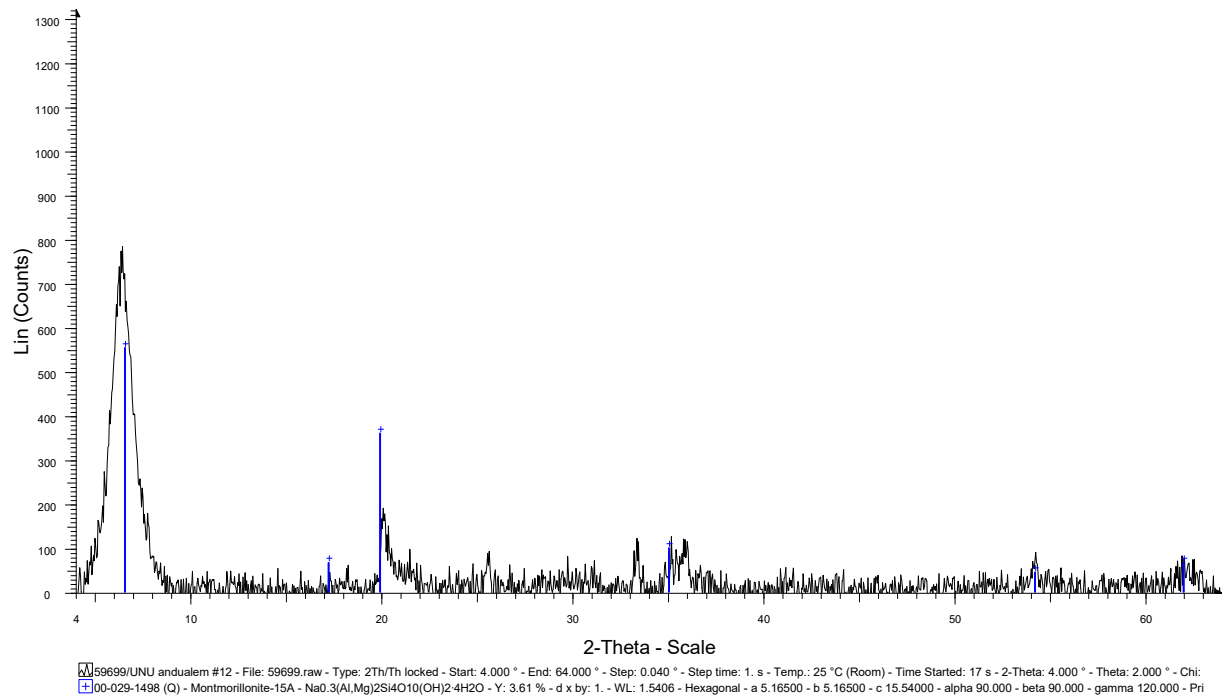


FIGURE 7: XRD graph indicating the presence of smectite clay minerals in sample 12 collected from around the fossil or extinct alteration at locality GR-10